EXPERIMENTAL AND NUMERICAL INVESTIGATIONS OF THE THERMAL PERFORMANCES OF WICKLESS HEAT PIPES USING NANOFLUIDS

Associate Prof. ***Gabriela HUMINIC,*** *Associate Prof.* ***Angel HUMINIC***

„TRANSILVANIA“ UNIVERSITY OF BRAŞOV

Abstract. *In this work, a three-dimensional analysis is used to investigate the heat transfer of a wickless heat pipe using water and nanofluids as the working fluid. The study focused mainly on the effects of volume concentrations of nanoparticles and the operating temperature on the heat transfer performance of the wickless heat pipe using the nanofluids. The analysis was performed for water and* $\gamma - Fe_2O_3$ *nanoparticles, three volume concentrations of nanoparticles (0%, 2%vol. and 5.3%vol.) and six operating temperatures (50°C, 60°C, 70°C, 80°C, 90°C and 95°C. The numerical results show that the volume concentration of nanoparticles had a significant effect in reducing the temperature difference between the evaporator and condenser. Experimental and numerical results show qualitatively that the wickless heat pipe using the nanofluid has better heat transfer characteristics than the wickless heat pipe using water.*

Keywords*: Nanoparticle, nanofluids, wickless heat pipe, heat transfer.*

1. INTRODUCTION

As a new research frontier, nanofluid two-phase flow and thermal physics have the potential to improve heat transfer and energy efficiency in thermal management systems. It has been demonstrated that nanofluids can have remarkably higher thermal conductivities than those of conventional pure fluids and significantly better heat transfer characteristics than the base fluids. Moreover, heat pipes with nanofluids are not only of academic interest but also of industrial interest. Recently, the number of companies that observe the potential of the technology of heat pipes filled with nanofluids is increasing. In the realm of electronics cooling, some companies are conducting research to use nanofluids instead of water and in the automotive industry, nanocars, GM and Ford, among others are focusing on nanofluids research projects [1].Up to now, studies concerning application of nanofluids in heat pipes or wickless heat pipe are experimental and only a few reports the modeling of the heat pipe characteristics in the presence of a nanofluid.

Naphon et al. [2] researched the heat transfer performance of a thermosyphon using titanium–ethanol nanofluid and titanium–water nanofluid. The results showed that the work efficiency of the thermosyphon using nanofluids is improved by 40% compared with that of the thermosyphon using pure refrigerant R11.

Yang and Liu [3] performed an experimental study on the thermal performance of a thermosyphon using nanofluids under steady operating pressures. Water, functionalized nanofluid and traditional nanofluid (the nanofluid consisting of unfunctionalized nanoparticles) were used as working fluids. The thermosyphon was a rectangle thermosyphon made of copper with inner chamber size of 350× 100 × 8 mm and vertically oriented. Surface-functionalized silica nanoparticles were used to prepare a kind of stable nanofluid (called functionalized nanofluid). The experiment was carried out with different nanoparticles concentrations (0.5 wt%, 1.0 wt%, 1.5 wt% and 2.0 wt%) and different operating temperatures (40°C, 55°C and 70°C). The experimental results showed that the evaporating heat transfer coefficient of functionalized nanofluid increases maximally by 17% at the operating temperature of 40°C. Also, the maximum heat flux of functionalized nanofluid is quite close to that of water, which indicates that functionalized nanofluid have nearly no effects on the maximum heat flux enhancement.

In opposite, traditional nanofluid deteriorates the evaporating heat transfer coefficient, but enhances

the maximum heat transfer. Authors considered that these differences result from changes of the thermophysical properties in the case of functionalized nanofluid and the deposition layer on the heated surface for traditional nanofluid.

Parametthanuwat et al. [4] studied the heat transfer of nanofluid in a thermosyphon for economizer. Water, water-based silver nanofluid with silver concentration 0.5 w/v%, and the nanofluid (NF) mixed with 0.5, 1.0, and 1.5 w/v% of oleic acid (OA) were used as working fluids. Thermosyphon for econo`mizer consisting of evaporation, adiabatic and condensation sections with 250 mm × 250 mm × 250 mm in width, length and height. The authors investigated the effects the operating temperature (60, 70 and 80°C), the volumetric flow rate (1, 2 and 5 l/min), the filling ratio (30%, 50% and 80%) and the concentration of oleic acid surfactant in nanofluid (0, 0.5, 1.0 and 1.5 w/v%) on the heat transfer performance. Results showed that the thermosyphon efficiency can be enhanced by 30% at the volumetric flow rate of 1 l/min, the filling ratio of 50%, and the operating temperature of 80°C

Firouzfar et al. [5] investigated the effectiveness of the thermosyphon heat exchanger and energy saving enhancement with nanofluids. Methanol and methanol-silver nanofluid were used as working fluids. The experiment was carried out with a mass flow rate of 0.15 kg/s, nominal relative humidity of 60%, and filling ratio of 50% from of the evaporator volume. The experimental results showed that is possible to achieve energy saving around 8.8-31.5% for cooling and 18-100% for reheating of supply air with methanol-silver nanofluid as the working fluid.

Leong et al. [6] carried out to study the heat transfer performance of a thermosyphon heat recovery exchanger with water based alumina and water based titanium dioxide as working fluids. The length and the outer diameter of the test thermosyphon were 1300 mm and 15 mm respectively. The experimental results showed that the overall heat transfer coefficient of the thermosyphon operated with TiO_2 nanofluids is slightly higher than Al_2O_3 nanofluids. Also, the experiments have found that the change of nanofluid thermophysical properties hasn't a significant influence on heat transfer enhancement. The overall heat transfer coefficient of the thermosyphon can be enhanced by 23% for 4 vol.% TiO_2 and 7 vol.% Al_2O_3 nanofluids when hot air velocity increases from 2.5 m/s to 4.75 m/s.

Lu et al. [7] performed an experimental study on the thermal performance of the open thermosyphon using the deionized water and water-based CuO nanofluids as the working liquid.

The tubular evaporator was made of a cooper tube with the total length and inner diameter of the evaporator tube was 1750 mm and 36 mm respectively. The authors investigated the effects of filling rate, nanoparticle mass concentration, and the operating temperature on the evaporating heat transfer characteristics in the open thermosyphon. The experimental results showed that adding nanoparticles to the base fluid significantly improved the thermal performance of the thermosyphon at the mass concentration of 1.2 wt.% and the filling ratio of 60% for maximal heat transfer enhancement.

Shanbedi et al. [8] investigated the effect of addition of multiwalled carbon nanotubes (MWCNTs) functionalized with ethylenediamine (EDA) to deionized water (DI water) on the heat-transfer performance of a two-phase closed thermosyphon. The experiments carried out for different input powers (30–150 W) and the various weight concentrations (0.2%–1.5%). The experimental results showed that for EDA-MWCNT/DI-water nanofluid with a concentration of 1% by weight and an input power of 90 W, the thermal efficiency can be enhanced by 93%.

Huminic [9, 10] studied the heat transfer characteristic of thermosyphon used iron oxide-water nanofluids with the nanoparticles volume concentration of 0%, 2%, and 5.3%. The thermosyphon heat pipe is a copper tube with the diameter and length of 15 mm and 2000 mm, respectively. Effects of thermosyphon inclination angle, operating temperature and nanoparticles concentration levels on the heat transfer characteristics of the thermosyphon are investigated. The results showed that the operating temperature and the inclination tilt had effects on the heat transfer rate of the TPCT, and also, the heat transfer rate using iron oxide nanoparticles at all concentrations were higher than with pure water.

Yang and Liu [11] investigated the effect of the operating pressure, the mass concentration of nanoparticles and the heated surface morphology on the boiling heat transfer in the loop thermosyphon. Results indicate that flow boiling heat transfer in the evaporator of the thermosyphon loop can be enhanced by adding CuO nanoparticles into water and the CHF enhancement ratio of the nanofluid increases with increasing pressure and with increasing mass concentration of nanoparticles when the nanoparticle mass concentration is less than 1.0 wt%. Moreover, the nanoparticle mass

concentration and the boiling time both affects the surface morphology of the coating surface formed after the boiling of nanofluids. Also, the operating pressure has no meaningful effect on the surface morphology of the coating surface

Shafahi et al. [12] used a two-dimensional model to simulate the thermal performance of the cylindrical heat pipes [11] and flat-shaped heat pipes [13] using nanofluids. Water, Al2O3-water, CuO-water and TiO2-water were tested as working fluids. The concentration of the nanoparticles was varied from 1% to 4% of the volume of the base fluid. The numerical results showed that increasing the nanoparticles concentration decreases the temperature difference between the evaporator and condenser and the thermal resistance.

Based on the previous researches concerning the use of nanofluids on the wickless heat pipes, the present study focused on experimental and numerical investigations of the thermal performances of the wickless heat pipes with water and $\gamma - Fe_2O_3$ nanoparticles and the volume concentration of 2.0% and 5.3%. Three-dimensional analysis of the wickless heat pipes were investigated under two-phase flow conditions and obtained results will be validated with the experimental results.

2. PREPARATION OF NANOFLUIDS

The test nanofluids were obtained by dispersing $\gamma - Fe_2O_3$ nanoparticles in pure water. The $\gamma - Fe_2O_3$ nanoparticles, with mean sizes of about 4-5 nm were prepared by the CO_2 laser co-pyrolysis of iron pentacarbonyl $Fe(CO)_5$ (vapors) and air. The method is based on the resonance between the emission of a continuous-wave CO_2 laser line and the infrared absorption band of a gas precursor and on subsequent heating of precursors by collisional energy transfer. The synthesis has been carried out in a flow reactor that has been described in detail earlier. After synthesis, the morphology and composition of the nanocomposites were characterized by different analytical techniques: X-ray diffraction (XRD), transmission electron microscopy (TEM), selected area electron diffraction (SAED) and high-resolution transmission electron microscopy (HRTEM). High-resolution transmission electron microscopy analysis was performed on many different domains of the nanocomposite and is presented in Figure 1. More detailed description of the analysis methods was presented in Ref. [10].

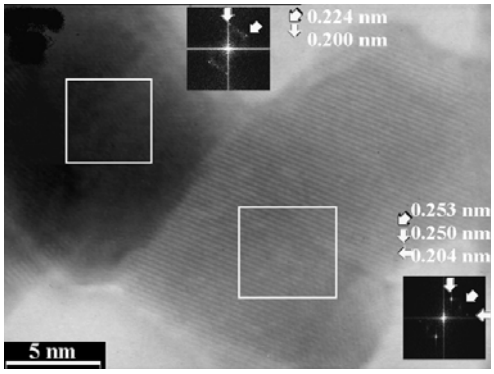

Fig. 1. HRTEM images, for the iron oxide sample: (*a*) isolated monocrystals, showing the separation interface and (*b*) agglomerated nanoparticles. In both images, space representations of Fourier transform are displayed.

3. EXPERIMENTAL APPARATUS AND PROCEDURE

The wickless heat pipe is made of copper tube with outer diameter of 15 mm, 0.7 mm thickness and 2000 mm in length. The evaporator and condenser sections had 850 and 850 mm length, respectively. Experiments were conducted in following conditions: the temperature of the heating water from the evaporator section was kept constant by a thermostatic bath (GD 120-S26) and the operating temperature was varied between 50 and 95 °C; the temperature of the cooling water from the condenser was kept constant at 20 °C through a thermostatic bath; the tested concentration level of nanoparticles is 0%, 2%, and 5.3%.

Descriptions of the experimental apparatus and the procedure for studying the heat transfer performance of nanofluids inside a wickless heat pipe with nanofluids can be found in Ref. [10].

4. MATHEMATICAL FORMULATION

The flow fluid and heat transfer into heat pipe is a process very complex. In consequence, the efficiency of a thermal CFD simulation depends on many factors. Creation of the model geometry and its integration in a physical domain, grid generation and choice of a suitable numerical computing scheme are significant factors that can determine the level of success of the simulation process.

The CFD code used for this study was ANSYS CFX-12.0, which is fully integrated fluid analysis software of ANSYS Workbench platform (ANSYS Inc., Canonsburg, PA, USA). It combines CAD (modeling and input), complex meshing solutions, fast solution algorithm and post-processing facilities [14]. The hardware on which were conducted

the analyses is a parallel computer system of distributed memory (cluster) and it is composed of 20 processor cores with 150 GB memory RAM.

4.1. Thermophysical properties of nanofluids

Thermo-physical and transport properties of nanofluids are very important in the study of nanofluid two-phase flow and thermal physics. Temperature dependency of different physical properties (k, Cp, ρ, μ) of the working fluids has been considered to improve the accuracy of the calculations.

Thermal conductivity is an important property which has a major role in heat transfer with nanofluids. The Hamilton-Crosser correlation [15] with an empirical scaling factor was used for the determination of the nanofluid effective thermal conductivity as follows:

$$k_{\mathrm{NF}} = \mathrm{k}_{\mathrm{BF}} \left[\frac{k_{NP} + (n-1)k_{BF} - (n-1)\varphi\left(k_{BF} - k_{NP}\right)}{k_{NP} + (n-1)k_{BF} + \varphi\left(k_{BF} - k_{NP}\right)} \right] \tag{1}$$

where the empirical scaling factor given by $n = \frac{3}{\psi}$ and ψ is sphericity that takes into account the effect of different particle shapes on thermal conductivity. Since the nanoparticles used in this investigation are spherical, the shape factor ψ is 1.

Brinkman's equation can be used for estimation of nanofluid viscosity [16]:

$$\mu_{NF} = \frac{\mu_{BF}}{(1-\varphi)^{2.5}} \tag{2}$$

Specific heat of nanofluid was estimated by equation [17]

$$c_{\mathrm{p,NF}} = \frac{(1-\varphi)\left(\rho c_p\right)_{BF} + \varphi\left(\rho c_p\right)_p}{(1-\varphi)\rho_{BF} + \varphi\rho_p} \tag{3}$$

and the density of nanofluid was calculated from Eq. (4) [18]:

$$\rho_{\mathrm{NF}} = (1-\varphi)\rho_{\mathrm{BF}} + \varphi\rho_p \tag{4}$$

4.2. Governing equations

The governing equations for flow and heat transfer inside of the heat pipes were solved in the Cartesian coordinate system. The set of equations solved by ANSYS CFX are the unsteady Navier-Stokes equations in their conservation form [14].

The continuity equation:

$$\frac{\partial \rho}{\partial t} + \nabla \cdot \left(\rho U\right) = 0 \tag{5}$$

The momentum equation:

$$\begin{aligned} \frac{\partial \rho U}{\partial t} + \nabla \cdot \left(\rho U \otimes U\right) &= -\nabla p + \nabla \cdot \tau + S_M = \\ &= \nabla \cdot \left(-p\delta + \mu(\nabla U + (\nabla U)^T\right) + S_M \end{aligned} \tag{6}$$

The total energy equation:

$$\begin{aligned} \frac{\partial \rho h_{tot}}{\partial t} - \frac{\partial p}{\partial t} + \nabla \cdot \left(\rho U h_{tot}\right) = \\ = \nabla \cdot \left(\lambda \nabla T\right) + \nabla \cdot \left(U \cdot \tau\right) + U \cdot S_M + S_E \end{aligned} \tag{7}$$

The term $\nabla \cdot \left(U \cdot \tau\right)$ represents the work due to viscous stresses and is called the viscous work term.

The term $U \cdot S_M$ represents the work due to external momentum sources and is currently neglected.

4.3. Grid resolution and boundary conditions

ANSYS CFX uses an element-based finite volume method, which first involves discretizing the spatial domain using a mesh. The mesh is used to construct finite volumes, which are used to conserve relevant quantities such as mass, momentum, and energy. In this work the grid was generated using a multi-block scheme, with tetrahedral elements and wedges elements nearest to surface of the heat exchanger in order to solve accurately the flow in the proximity of the later. Thus, the dimensions of the computational grid were:

– global number of grid points: 240,720;

– global number of elements: 154,000.

According with previously mentioned, the boundary conditions of the processes were following:

– inlet: axial velocity and volume fraction were imposed;

– outlet: zero pressure condition, P =0 was considered;

– wall: temperature was imposed;

– for the interference surfaces of the domains, conservative interface flux was considered.

For all simulations performed in the present study, converged solutions were considered when the residuals resulting from an iterative process were lower than 10^{-5}. Also, the high-resolution advection scheme was selected for the simulations and the double-precision solver was used.

5. RESULTS AND DISCUSSION

In the present analysis, the numerical simulations are performed for six of the operating temperatures of the wickless heat pipe (50°C, 60°C, 70°C, 80°C, 90°C and 95°C)) and two nanoparticles concentrations (2. vol% and 5.3 vol.%).

In order to quantitatively evaluate the thermal performance of the heat pipes, the temperature profiles of the wickless heat pipes using both water and the nanofluids are compared. Figsures 2-7 show the wall temperature distribution along of the wickless heat pipe for different operating temperatures and different nanoparticles concentration.

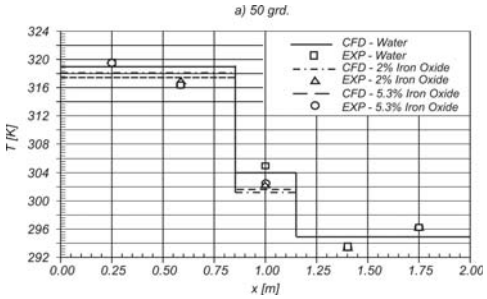

Fig. 2. Wickless heat pipe temperature distribution for different nanoparticles concentrations and an operating temperature T = 50°C.

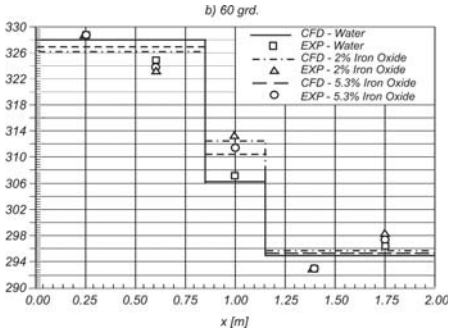

Fig. 3. Wickless heat pipe temperature distribution for different nanoparticles concentrations and an operating temperature T = 60°C.

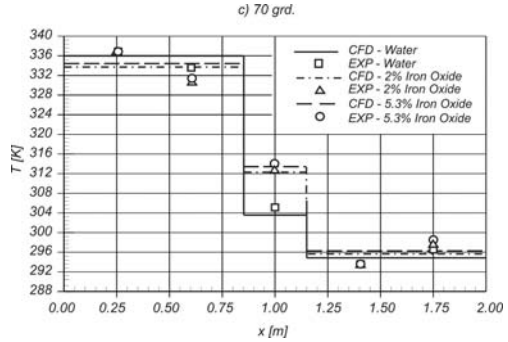

Fig. 4. Wickless heat pipe temperature distribution for different nanoparticles concentrations and an operating temperature T = 70°C.

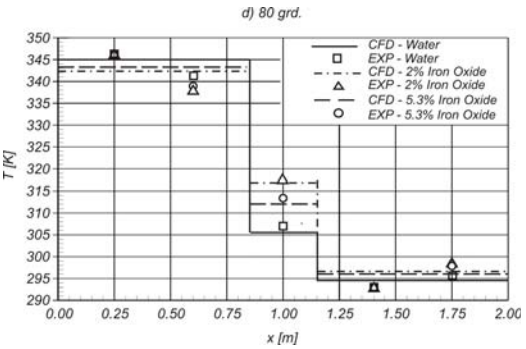

Fig. 5. Wickless heat pipe temperature distribution for different nanoparticles concentrations and an operating temperature T = 80°C.

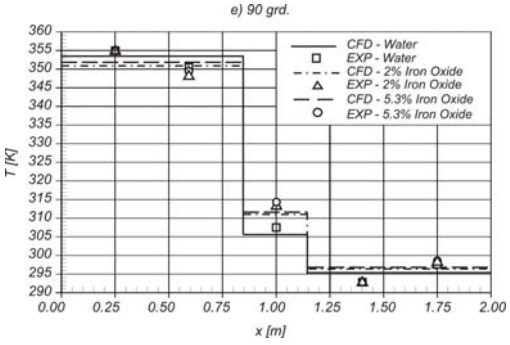

Fig. 6. Wickless heat pipe temperature distribution for different nanoparticles concentrations and an operating temperature T = 90°C.

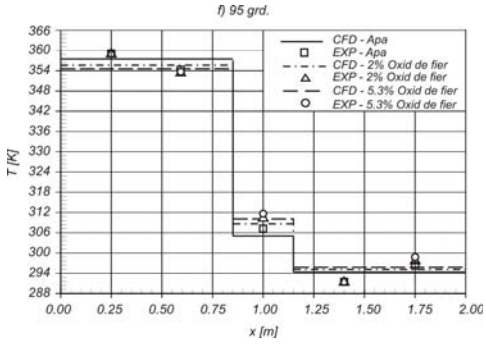

Fig. 7. Wickless heat pipe temperature distribution for different nanoparticles concentrations and an operating temperature T = 95°C.

Temperature distribution results are compared with the experimental results [10] and were found to be in very good agreement. As seen in these figures, the temperatures significantly decrease on evaporator when are used nanofluids as working fluid. Also, increases the particle concentration decrease the temperature difference between the evaporator and condenser sections. Experimental and numerical results show qualitatively that the wickless heat pipe using the nanofluid has better

heat transfer characteristics than the wickless heat pipe using water.

Figure 8 shows the comparison of the total heat resistances of the thermosyphon heat pipe with the nanofluids and water. It can be seen that increasing the nanoparticle concentration decreases the thermal resistance of thermosyphon heat pipe thus providing a better performance.

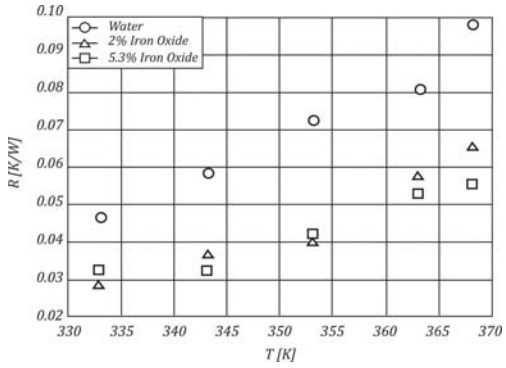

Fig. 8. Effect of iron oxide nanoparticles on total thermal resistance of the wickless heat pipe.

6. CONCLUSIONS

In this paper the thermal behaviour of water and nanofluids flowing inside a wickless heat pipe was numerically investigated in stationary conditions and for laminar flow. The wickless heat pipe temperature profiles are obtained for different volume concentrations of nanoparticles and different operating temperatures of the wickless heat pipe. The results have showed that the heat transfer behaviors of the nanofluids were highly depended on the volume concentration of nanoparticles and weakly dependent on the temperature. Also, the numerical results confirm experimental results obtained so far as well as the thermal performances of the wickless heat pipes are improved and the temperature difference between the evaporator and condenser is reduced when nanofluids are used as the working fluid.

NOMENCLATURE

c_p	specific heat [J/kg K]
h	specific enthalpy [J/kg]
k	thermal conductivity [W/mK]
P	pressure [Pa]
R	thermal resistance [K/W]
T	temperature [K]
t	time [s]
U	vector of velocity [m/s]
S_E	energy source [kg/m s^3]
S_M	momentum source [kg/m^2 s^2]

Operators

$\otimes$	tensor multiplication
∇	gradient
$\nabla\cdot$	divergence

Greek symbols

φ	volume concentration
δ	identity matrix
λ	second coefficient of viscosity
μ	dynamic viscosity [N s/m^2]
ρ	density [kg/m^3]
τ	stress tensor
σ	surface tension [N/m]

Subscripts

BF	base fluid
NF	nanofluid
p	particle

ACKNOWLEDGMENTS

This work was supported by a grant of the Romanian National Authority for Scientific Research, CNCS – UEFISCDI, project number PN-II-ID-PCE-2011-3-0275.

REFERENCES

[1] Wang, X. Q., and Mujumdar, A. S., 2008, *A review on nanofluids – Part II: Experiments and applications,* Brazilian Journal of Chemical Engineering, 25(04), pp. 631 – 648.

[2] Naphon, P., Assadamongkol, P., and Borirak, T., 2008, *Experimental investigation of titanium nanofluids on the heat pipe thermal efficiency,* Int. Commun. Heat Mass Transfer, 35, pp. 1316–1319.

[3] Yang, X.F, and Liu, ZH., 2011, *Application of functionalized nanofluid in thermosyphon,*, Nanoscale Research Letters, 6, pp. 494.

[4] Parametthanuwat, T., Rittidech, S., Pattiya, A., Ding, Y., and Witharana, S., 2011, *Application of silver nanofluid containing oleic acid surfactant in a thermosyphon economizer,* Nanoscale Research Letters, 6, pp.315.

[5] Firouzfar, E, Soltanieh, M, Noie, S.H., and Saidi, S.H., 2011, *Energy saving in HVAC systems using nanofluid* , Applied Thermal Engineering , 31(8-9), pp.1543-1545.

[6] Leong, K.Y., Saidur, R., Mahlia, T.M.I., and Yau, Y.H., 2012, *Performance investigation of nanofluids as working fluid in a thermosyphon air preheater,* Int Commun. Heat Mass Transfer, 39(4), pp.523–529.

[7] Lu, L., Liu, Z.H., and Xiao, H.S., 2011, *Thermal performance of an open thermosyphon using nanofluids for high-temperature evacuated tubular solar collectors Part 1: Indoor experiment,* Solar Energy, 85(2), pp.379–387.

[8] Shanbedi, M., Zeinali Heris, S., Baniadam, M., Amiri, A., and Maghrebi, M., 2012, *Investigation of Heat-Transfer Characterization of EDA-MWCNT/DI-Water Nanofluid in a Two-Phase Closed Thermosyphon,* Industrial & Engineering Chemistry Research, 51(3), pp.1423–1428.

[9] Huminic, G., Huminic, A., Morjan, I., and Dumitrache, F., 2011, *Experimental study of the thermal performance of thermosyphon heat pipe using iron oxide nanoparticles,* Int. J. Heat Mass Transfer, 54, pp.656- 661.

[10] Huminic, G., and Huminic, A., 2011, *Heat transfer characteristics of a two-phase closed thermosyphons using nanofluids,* Experimental Thermal and Fluid Science, 35(3), pp.550-557.
[11] Yang, X.F., and Liu, Z.H., 2012, *Flow boiling heat transfer in the evaporator of a loop thermosyphon operating with CuO based aqueous nanofluid,* Int. J. Heat Mass Transfer, 55, pp.7375–7384.
[12] Shafahi, M., Bianco, V., Vafai, K., and Manca, O., 2010, *An investigation of the thermal performance of cylindrical heat pipes using nanofluids*, Int. J. Heat Mass Transfer, 53, pp.376-383.
[13] Shafahi, M., Bianco, V., Vafai, K., and Manca, O., 2010, *Thermal performance of flat-shaped heat pipes using nanofluids,* Int. J. Heat Mass Transfer, 53, pp. 1438-1445.
[14] *** *ANSYS CFX 14.0, Theory Book,* 2011, ANSYS Inc.
[15] Hamilton, R. L., and Crosser, O. K., 1962, *Thermal Conductivity of Heterogeneous Two Component Systems,* I & EC Fundament, 1, pp. 187–191.
[16] Brinkman, H.C., 1952, *The viscosity of concentrated suspensions and solution,* J. Chem. Phys., pp. 571–581.
[17] Xuan, Y., and Roetzel, W., 2000, *Conceptions for heat transfer correlation of nanofluid,* Int. J. Heat Mass Transfer, 43, pp.3701–3707.
[18] Pak, B.C., and Cho, Y.I., 1998, *Hydrodynamic and heat transfer study of dispersed fluids with submicron metallic oxide particles,* Exp. Heat Transfer, 11, pp.151–170.